for predicting tumors without vessel invasion in patients with adenocarcinoma of the lung.

At both baseline screenings and repeat CT screenings for lung cancer, tumors containing a nonsolid component have been found to be a significant sign of malignancy.[24] Henschke and colleagues[25] found that 19% of the 233 cases with positive results at baseline screening had a tumor with the nonsolid component and that the tumors were predominantly bronchioloalveolar carcinoma and adenocarcinoma with bronchioloalveolar carcinoma features. These predominant histologic types of malignancy corresponded to noninvasive and invasive tumors of lung adenocarcinoma. The quantification of the extent or growth rate of the solid and nonsolid components of tumors is necessary during CT scan screening for lung cancer.

Swensen and colleagues[18] created a multivariate logistic regression model to predict a malignant solitary pulmonary nodule (SPN) in a derivation and validation analysis. Of 629 radiologically intermediate nodules in their study, 23% were malignant SPNs. The investigators identified the following three independent findings that predicted malignant SPNs: upper lobe distribution; tumor size; and spiculation. Among these findings, spiculation was associated with the prediction model in our results. Pleural indentation and male predilection were also significant predictors of tumors with vessel invasion in our study.

Some studies[26–28] using the segmentation algorithm of software have yielded calculations of tumor volume in three dimensions. The excellent interobserver variability suggests that tumor volume estimations by different observers can be reliably compared when three-dimensional volumetric software is used. However, this technique does not enable the segmentation of tumors that contain a nonsolid component.[27,28] Since most tumors in our study contained a nonsolid component and were not appropriate for three-dimensional volumetric analysis, tumor volume was calculated by the perimeter method, which had potential sources of error that affected the results of volumetric analyses.[29]

The proportion occupied by the nonsolid component was dichotomized using the median value for a threshold level in the univariate and multivariate analyses performed. In both the univariate and multivariate analyses, the proportion occupied by the nonsolid component yielded the highest point estimates and CIs for the ORs of tumors without vessel invasion. However, it should be noted that there was enough of a difference between the values for patients in whom the nonsolid component occupied a high proportion of the tumor and those for patients in whom the nonsolid component occupied a small proportion of the tumor that similar results could have been obtained with different threshold values.

There are other potential limitations of this study. The size of the sample may also have led to false-positive results because of the number of covariates included in the initial analysis. However, the strength of the association with our primary outcome of interest, as well as the historical precedence of other significant predictors in our multivariate analysis, lends credence to our conclusions. In summary, the results of our study confirm that the proportion occupied by the nonsolid component of a tumor on CT scans is a reliable predictor of tumors without vessel invasion with much greater confidence than was possible in the past.

References

1 Travis WD, Colby TV, Corrin B, et al. Histological typing of lung and pleural tumors. Berlin, Germany: Springer, 1999

2 Noguchi M, Morikawa A, Kawasaki M, et al. Small adenocarcinoma of the lung: histologic characteristics and prognosis. Cancer 1995; 75:2844–2852

3 Jang HJ, Lee KS, Kwon OJ, et al. Bronchioloalveolar carcinoma: focal area of ground-glass attenuation at thin-section CT as an early sign. Radiology 1996; 199:485–488

4 Kuriyama K, Seto M, Kasugai T, et al. Ground-glass opacity on thin-section CT: value in differentiating subtypes of adenocarcinoma of the lung. AJR Am J Roentgenol 1999; 173:465–469

5 Ohde Y, Nagai K, Yoshida J, et al. The proportion of consolidation to ground-glass opacity on high resolution CT is a good predictor for distinguishing the population of non-invasive peripheral adenocarcinoma. Lung Cancer 2003; 42: 303–310

6 Aoki T, Tomoda Y, Watanabe H, et al. Peripheral lung adenocarcinoma: correlation of thin-section CT findings with histologic prognostic factors and survival. Radiology 2001; 220:803–809

7 Suzuki K, Yokose T, Yoshida J, et al. Prognostic significance of the size of central fibrosis in peripheral adenocarcinoma of the lung. Ann Thorac Surg 2000; 69:893–897

8 Kodama K, Higashiyama M, Yokouchi H, et al. Prognostic value of ground-glass opacity found in small lung adenocarcinoma on high-resolution CT scanning. Lung Cancer 2002; 33:17–25

9 Matsunaga H, Yokoi K, Anraku M, et al. Proportion of ground-glass opacity on high-resolution computed tomography in clinical T1N0M0 adenocarcinoma of the lung: a predictor of lymph node metastasis. J Thorac Cardiovasc Surg 2002; 124:278–284

10 Kim EA, Johkoh T, Lee KS, et al. Quantification of ground-glass opacity on high-resolution CT of small peripheral adenocarcinoma of the lung: pathologic and prognostic implications. AJR Am J Roentgenol 2001; 177:1417–1422

11 Takashima S, Maruyama Y, Hasegawa M, et al. Prognostic significance of high-resolution CT findings in small peripheral adenocarcinoma of the lung: a retrospective study on 64 patients. Lung Cancer 2002; 36:289–295

12 Lababede O, Meziane MA, Rice TW. TNM staging of lung cancer: a quick reference chart. Chest 1999; 115:233–235

13 Adler B, Padley S, Miller RR, et al. High-resolution CT of bronchioloalveolar carcinoma. AJR Am J Roentgenol 1992; 159:275–277

14 Winter-Muram HT, Jennings SG, Tarver RD, et al. Volumetric growth rate of stage I lung cancer prior to treatment: serial CT scanning. Radiology 2002; 223:798–805
15 Winter-Muram HT, Jennings SG, Meyer CA, et al. Effect of varying CT section width on volumetric measurement of lung tumors and application of compensatory equations. Radiology 2003; 229:184–194
16 Jennings SG, Winter-Muram HT, Tarver RD, et al. Lung tumor growth: assessment with CT-comparison of diameter and cross-sectional area with volume measurements. Radiology 2004; 231:866–871
17 Hanley JA, McNeil BJ. The meaning and use of the area under a receiver operating characteristic (ROC) curve. Radiology 1982; 143:29–36
18 Swensen SJ, Silverstein MD, Ilstrup DM, et al. The probability of malignancy in solitary pulmonary nodules: application to small radiologically intermediate nodules. Arch Intern Med 1997; 157:849–855
19 Lemeshow S, Hosmer DW. A review of goodness-of-fit statistics for use in the development of logistic regression models. Am J Epidemiol 1982; 115:92–106
20 Wasson JH, Sox HC, Neff RK, et al. Clinical prediction rules: applications and methodological standards. N Engl J Med 1985; 313:793–799
21 Scott JA. Pulmonary perfusion patterns and pulmonary arterial pressure. Radiology 2002; 224:513–518
22 Arana E, Delicado P, Marti-Bormati L. Validation procedures in radiologic diagnostic models: neural network and logistic regression. Invest Radiol 1999; 34:636–642
23 Stone M. Cross-validatory choice and assessment of statistical predictions. J R Stat Soc B 1974; 36:111–147
24 Henschke CI, McCauley DI, Yankelevitz DF, et al. Early lung cancer action project: overall design and findings from baseline screening. Lancet 1999; 354:99–105
25 Henschke CI, Yankelevitz DF, Mircheva R, et al. CT screening for lung cancer: frequency and significance of part-solid and nonsolid nodules. AJR Am J Roentgenol 2002; 1178: 1053–1057
26 Yankelevitz DF, Reeves AP, Kostis WJ, et al. Small pulmonary nodules: volumetrically determined growth rates based on CT evaluation. Radiology 2000; 217:251–256
27 Revel MP, Lefort C, Bissery A, et al. Pulmonary nodules: preliminary experience with three-dimensional evaluation. Radiology 2004; 231:459–466
28 Revel MP, Bissery A, Bienvenu M, et al. Are two-dimensional CT measurements of small noncalcified pulmonary nodules reliable? Radiology 2004; 231:453–458
29 Staron RB, Ford E. Computed tomographic volumetric calcification reproducibility. Invest Radiol 1986; 21:272–274

Skelet Radiol
DOI 10.1007/s00256-005-0021-0

SCIENTIFIC ARTICLE

Ukihide Tateishi
Tadashi Hasegawa
Takayuki Nojima
Tsutomu Takegami
Yasuaki Arai

MRI features of extraskeletal myxoid chondrosarcoma

Received: 23 February 2005
Revised: 13 May 2005
Accepted: 27 July 2005

All authors of this research paper have directly participated in the planning, execution, or analysis of the study
The contents of this manuscript have not been copyrighted or previously published
There are no directly related manuscripts or abstracts, published or unpublished, by any authors of this paper

U. Tateishi (✉) · Y. Arai
Division of Diagnostic Radiology,
National Cancer Center Hospital,
5-1-1, Tsukiji, Chuo-Ku,
104-0045 Tokyo, Japan
e-mail: utateish@ncc.go.jp
Tel.: +81-3-35422511
Fax: +81-3-35423815

T. Hasegawa
Department of Clinical Pathology,
Sapporo Medical University
School of Medicine,
Sapporo, Japan

T. Nojima
Department of Pathology,
Kanazawa Medical University,
Ishikawa, Japan

T. Takegami
Division of Molecular Oncology
and Virology,
Medical Research Institute,
Kanazawa Medical University,
Ishikawa, Japan

Abstract *Objective:* To describe the MRI features of extraskeletal myxoid chondrosarcoma in comparison with clinicopathologic findings. *Design and patients:* The study comprised 12 male subjects and seven female subjects with a mean age of 53 years (range 16–76 years). MRI findings, evaluated by two radiologists with agreement by consensus, were compared for histopathologic features. *Results:* The tumor size ranged from 2.0 cm to 20.0 cm (mean 8.9 cm). Fusion gene transcripts could be detected in 13 (68%) of the 19 cases: EWS-CHN in nine cases, TAF2N-CHN in three, and TFG-TCH in one. There were six fusion-negative cases. Signal characteristics on T1-weighted and T2-weighted MR images were non-specific with regard to each cytogenetic variant. Peripheral enhancement was seen more frequently in tumors with the EWS-CHN variant than in those with other cytogenetic variants. The characteristic pattern of enhancement corresponded to the presence of fibrous septa and peripheral areas of high cellularity within lobules, by correlation with pathologic findings. All cases with TAF2N-CHN or TFG-TCH variants showed invasion of extracompartmental structure, bone, or vessels. *Conclusion:* Extraskeletal myxoid chondrosarcoma is an uncommon soft-tissue malignancy that may be recognized by MRI features of multilobular soft-tissue mass often invading extracompartmental, bony, and vascular structures.

Keywords Extraskeletal myxoid chondrosarcoma · MRI · Cytogenetic variant

Introduction

Extraskeletal myxoid chondrosarcoma (EMC) is a rare malignant soft-tissue tumor characterized by abundant myxoid matrix and malignant chondroblastic cells [1, 2]. EMC mostly arises in the deep soft tissue of the proximal extremities and limb girdles and comprises multiple gelatinous nodules divided by fibrous septa. Although the most common manifestation is an enlarging soft-tissue mass, some lesions are accompanied by pain and tenderness or may restrict the range of motion. Long-term follow-up studies have shown that EMC is a slowly growing tumor with a risk of local recurrence or distant metastasis. EMC is a tumor with long survival but is known to have a potential for local recurrence, metastasis, and a disease-associated death [1–4].

EMC was described as a distinct entity, precisely, by Enzinger and Shiraki [5]. Subsequent clinicopathologic

and molecular studies have yielded findings consistent with the distinct tumor characteristics and have revealed that EMC is composed of at least four cytogenetic variants: EWS-CHN, TAF2N-CHN, TCF12-CHN, TFG-TCH [6–11]. These variants were derived from independent chromosomal translocations and the resultant fusion genes. The identification of the highly specific balanced chromosomal rearrangement in EMC assists a specific diagnosis at molecular level.

The typical radiographic manifestation of EMC is that of a large, well-demarcated mass, partially contained by pseudocapsule, with associated intratumoral cysts and hemorrhage. A few reports on case series of EMC had been published at the time this article was written [12–14]. In addition, the relationship between cytogenetic variants and imaging findings were not fully understood.

The purpose of our study was to describe the imaging features of EMC in comparison with clinicopathologic findings.

Materials and methods

Nineteen cases of EMC were retrieved from the pathology files of our institute. Patients were identified from a pathologic registration system database through a query for patients with diagnosed EMC who had undergone surgical resection. A reference pathologist reviewed all cases to confirm the histologic diagnosis based on current standards. Clinical information was extracted from the patient files regarding patient age, gender, symptoms, treatment, local recurrences, metastases, metastatic sites, associated conditions, and final disease status. Our institutional review board does not require its approval or patients' informed consent for this type of review.

Radiologic studies of each lesion were reviewed by two radiologists, with consensus, and included CT, with (n=4) and without (n=15) contrast material enhancement, and MRI with high-field (1.5-T) units in all patients. T1-weighted and T2-weighted images were obtained in the transverse plane and in at least one longitudinal plane with either a surface coil (n=15) or a body coil (n=4). T1-weighted fast spin-echo images were obtained by using a 24–30 cm field of view, 4–8 mm section thickness, 400–620 ms/8.9–15 ms repetition time/echo time, 256×192–224 matrix, two signals acquired. T2-weighted fast spin-echo acquisitions were performed by using a 24–35 cm field of view, 4–8 mm section thickness, 3,000–6,220 ms/84–120 ms repetition time/echo time, 256×192–224 matrix, two signals acquired. After the intravenous administration of 0.1 mmol of gadopentate dimeglumine (Magnevist, Schering, Berlin, Germany) per kilogram of body weight, transverse T1-weighted images with fat suppression were obtained in the transverse plane and in at least one longitudinal plane.

Images were evaluated for lesion location and size, depth (superficial or deep), shape of margin (well-defined or ill-defined), and the presence or absence of extracompartmental extension. Mineralized matrix was assessed on CT images. MR images were evaluated for predominant signal intensity characteristics (low, intermediate, or high), signal homogeneity or heterogeneity, as well as enhancement characteristics. On T1-weighted images low signal intensity was defined as signal intensity less than that of muscle; intermediate signal intensity, similar to that of muscle; and high signal intensity, similar to that of fat. On T2-weighted images, low signal intensity was defined as signal intensity similar to that of muscle; intermediate signal intensity, greater than that of muscle but less than that of fat; and high signal intensity, equal to or greater than that of fat. Tumor enhancement was visually graded as greater than, less than, or equal to, that of surrounding muscle and vessels. The pattern and homogeneity of enhancement were also recorded: peripheral, diffuse, and mixed patterns. Peripheral enhancement was assigned when the curvilinear enhancing septal areas were present within tumor. Cortical destruction and vascular encasement were also evaluated.

For reverse-transcribed polymerase chain reaction (RT-PCR) analysis, frozen tissues were available from 18 patients. The RNA was reverse transcribed, and the samples were then subjected to protein chain reaction (PCR) amplification using primers: CCCACTAGTTACCCAC CCCA (EWS exon 7 forward); TCTGGCAGACTTCTTT TAAGCA (EWS exon 11 forward); GCGATGCCACAGT GTCCTATG (EWS exon 12 forward); GAGCAGTCAA ATTATGATCAGCAGC (TAF2N forward); GCAACA ACGCATGGCCGCTAT (TCF12 forward); AGCTTGG AACCACCTGGAGAACC (TFG forward); GCTGTAT GTCTGCGCCGCATAACT (CHN-1 reverse); TCTCAG CCTCCGCTGGAGAGA (CHN-2 reverse). Specimens were fixed with formalin and sectioned in the same plane as that of the CT and MR images. The specimens were stained with hematoxylin–eosin, and immunohistochemical staining was also performed. In one patient whose frozen tissue was not available, fluorescence in situ hybridization (FISH) was performed to detect EWS gene aberrations in formalin-fixed paraffin-embedded tissue. Tumor specimens were immunostained with the antibody Ki-67 (Dako; diluted 1:100 and autoclaved), and the Ki-67 (MIB-1) labeling index (LI) was estimated by determining the percentage of Ki-67-positive cell nuclei per 1,000 tumor cells in the region of the tumor with the greatest density of ki-67 staining viewed under a light microscope. Both MIB-1 grade (MIB-1 grading system) and mitosis grade (the modified French system) are three-grade systems obtained by summing the scores of tumor differentiation, tumor necrosis, and the MIB-1 score or mitotic score, each of which was given a score of 0, 1, 2,or 3. Tumor differentiation score, according to histologic type, was modified slightly from the French system. The mitotic figures were counted on routine hematoxylin and eosin

Table 1 Cytogenetic variants of EMC (*T1WI* T1-weighted image, *T2WI* T2-weighted image, *NOS* not otherwise specified

Variant	Translocation	Number	T1WI	T2WI	Gadolinium enhancement	Extracompartmental extension	Bone invasion	Vascular invasion
EWS-CHN	t(9;22) (q22;q12)	9	Intermediate: 6 High: 3	Intermediate: 1 High: 8	Peripheral: 5 Mixed: 4	2	3	1
TAF2N-CHN	t(9;17) (q22;q11)	3	Intermediate: 2 High: 1	High: 3	Diffuse: 2 Mixed: 1	2	0	1
TFG-TCH	t(3;9) (q11;q22)	1	High: 1	Intermediate: 1	Mixed: 1	0	1	0
NOS	–	6	Intermediate: 6	Intermediate: 2 High: 4	Mixed: 3 Diffuse: 2 Peripheral: 1	1	1	2

stained sections. The areas selected for cell counting were from the most mitotically active parts of the tumors, usually located at the periphery. The mitotic score was assessed by counting the number of mitotic figures in ten consecutive high-power fields. The MIB-1 score was estimated by counting the percentage of MIB-1-positive cell nuclei per 1,000 tumor cells in the region of the tumor with the greatest density of staining, which, in most instances, corresponded to the areas with the highest mitotic activity. In this study the histological grade of a tumor was determined by a three-grade system in which tumor differentiation, tumor necrosis, and MIB-1 LI, were each given a score of 0, 1, 2, or 3 and then added together. Lesions with MIB-1 LIs of 0–9%, 10–29%, or greater than 30% were assigned MIB-1 scores of 1,2 or 3, respectively. The three separate scores were added together to produce a combined grade: lesions with a total score of 2 or 3 were classified as grade 1, those that scored 4 or 5 were grade 2, and those that scored 6,7 or 8 were grade 3. According to this MIB-1 system, tumors were assigned grades 1–3. The cut surface, internal characteristics, and microscopic findings of the lesions were compared with those seen on CT and MR images. Correlation between the imaging and histologic findings was made by consensus between the radiologist and pathologist.

Follow-up information was available in all cases. Deaths confirmed to be caused by disease were treated as an end point, whereas deaths from other causes were treated as censored observations. The disease-free date was considered to be the date when the medical record documented no

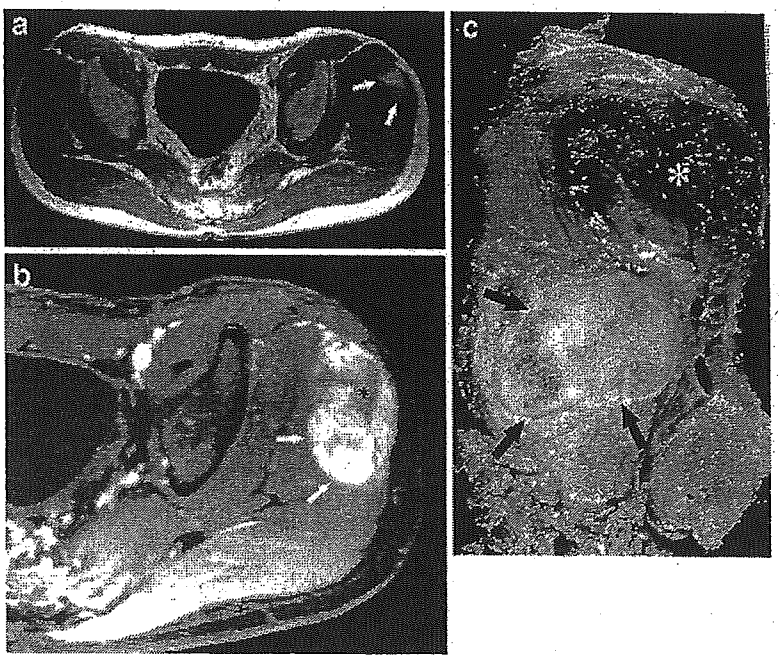

Fig. 1 A 46-year-old man with the TAF2N-CHN variant of EMC arising from the left gluteal region. **a** Transverse, T1-weighted (500 ms/15 ms), MR image shows a focus of high signal intensity within the tumor (*arrows*), resulting from hemorrhage. **b** Transverse, fat-saturated, T1-weighted (600 ms/12 ms), MR image after contrast enhancement demonstrates moderate enhancement of the tumor. The enhancement of hemorrhagic areas (*asterisk*) was depicted more heterogeneously than those of solid portions (*arrows*). **C** Sectioned gross specimen reveals hemorrhagic areas (*asterisk*) and solid portions (*arrows*) admixed with extensive myxoid stroma corresponding to the MRI appearance

evidence of disease. Recurrence was assigned when the patient developed recurrent tumor related to surgical margins. Metastasis was assigned when the patient developed distant a metastasis, including bone and lung metastases, during the course of the disease and did not contain the case with recurrence.

Results

There were 12 male (63%) and seven female (37%) patients aged from 16 years to 76 years, with an average age of 53 years. The arising sites of soft-tissues were calf (n=5), foot (n=4), buttock (n=3), thigh (n=3), groin (n=1), shoulder (n=1), arm (n=1), and hand (n=1). Presenting symptoms were stated in all patients. The most common symptom was a mass that had enlarged (n=15). Four patients had evidence of pain or tenderness. There were three cytogenetic variants in 13 cases (68%): EWS-CHN in nine cases, TAF2N-CHN in three, and TFG-TCH in one, and not otherwise specified in six cases (Table 1). There were 11 grade 1 tumors and eight grade 2 tumors as assigned by the MIB-1 grading system.

The mean diameter of tumors was 8.9 cm (range 2.0–20.0 cm). The location of the tumor was superficial in four patients (27%), while the remaining 11 (73%) were distributed deeply. Mineralized matrix that was centrally located within the tumor was seen in one case on non-enhanced CT images. Multi-nodular soft-tissue masses with well-defined (n=5, 26%) or ill-defined (n=14, 74%) margins were seen on CT and MR images. One patient (5%) demonstrated a metastatic lesion at initial presentation.

MR images showed predominantly intermediate (n=14, 74%) and high (n=5, 26%) signal intensity relative to muscle on T1-weighted MR images, with one lesion also demonstrating areas of focal high signal intensity, reflecting the hemorrhagic region (Fig. 1). On T2-weighted MR images, signal intensity was heterogeneous in all patients. Fifteen lesions (79%) had high signal intensity, equal to or greater than that of fat. The remaining four lesions (21%) had intermediate signal intensity, greater than that of muscle but less than that of fat. Signal characteristics on T1-weighted and T2-weighted MR images were non-specific with regard to each cytogenetic variant.

All lesions demonstrated mild-to-moderate and heterogeneous enhancement of the tumor after intravenous administration of a gadolinium-based contrast agent. Solid components of the tumors showed peripheral enhancement (n=6, 32%, Fig. 2), diffuse enhancement (n=4, 21%, Fig. 3), and a mixed pattern of enhancement (n=9, 47%). Peripheral enhancement was seen more frequently in tumors with the EWS-CHN variant than in those with other cytogenetic variants (P<0.05).

Ulceration of the tumor surface was identified in one case. Vascular encasement was seen in four cases, and one of those cases was accompanied by intravenous tumor extension. Tumors showed extracompartmental extension in five patients. Cortical destruction with soft-tissue mass was seen in five patients. Of these, a tumor arising from the back showed intraforaminal extension to the spinal canal, with marked bone destruction. All cases with TAF2N-CHN

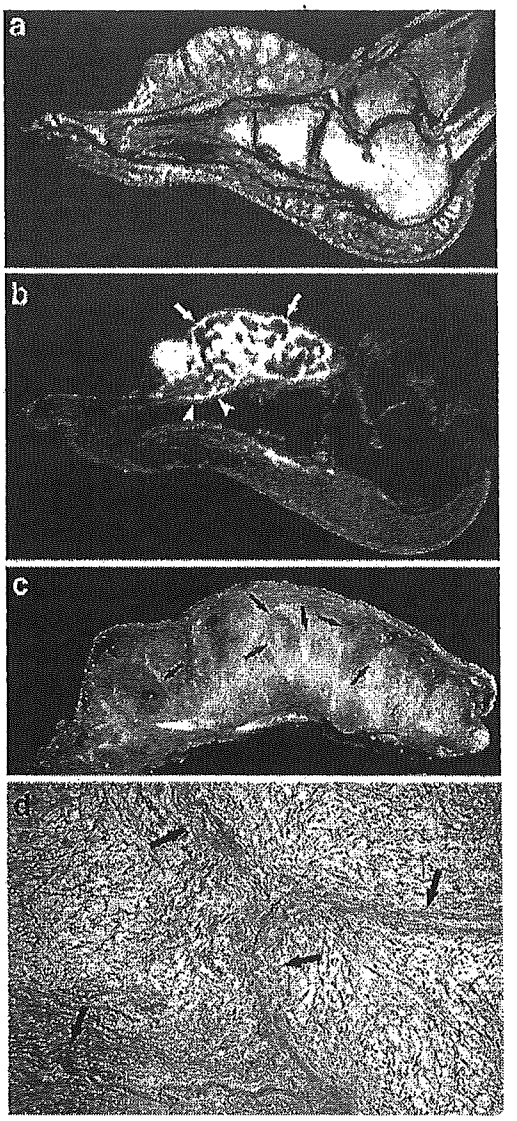

Fig. 2 A 76-year-old woman with the EWS-CHN variant of EMC of the foot. **a** Sagittal, T2-weighted (3,000 ms/102 ms), MR image shows a well-defined mass, involving the foot, with high signal intensity greater than that of subcutaneous fat. **b** Sagittal, fat-saturated, T1-weighted (600 ms/15 ms), MR image after contrast administration shows peripheral enhancement (*arrows*). Also noted is extracompartmental growth beyond fascia (*arrowheads*). **c** Sagittally sectioned gross specimen shows myxoid and gelatinous nodules separated by fibrous septa (*arrows*). **d** Photomicrograph of the specimen demonstrates mature hyaline cartilage with fibrous tissue and myxoid stroma corresponding to the MRI appearance (H & E, original magnification ×100)

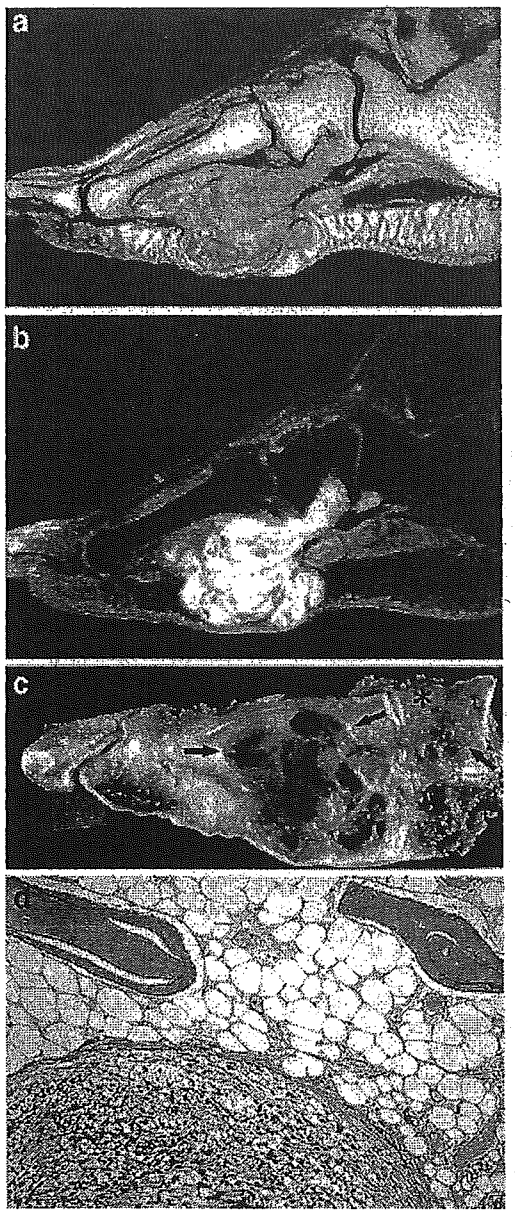

Fig. 3 A 61-year-old woman with the TFG-TCH variant of EMC manifesting as extracompartmental extension. **a** Sagittal, T2-weighted (4,000 ms/89.9 ms), MR image shows a poorly defined mass involving the sole, with intermediate signal intensity less than that of subcutaneous fat. **b** Sagittal, fat-saturated, T1-weighted (600 ms/15 ms), MR image after administration of contrast material shows diffuse enhancement. **c** Sagittal plane of pathology specimen reveals extracompartmental growth (*arrows*) and destruction of calcaneous bone (*asterisk*). **d** Photomicrograph of the specimen shows nodular architecture of marrow invasion (H & E, original magnification ×100)

or TFG-TCH variants showed invasion of extracompartmental structure, bone, or vessels.

Gross characteristics of resected specimens featured multi-nodular architecture corresponding to the cross-sectional MRI features. In all cases the cut surface of specimens revealed myxoid and gelatinous nodules separated by fibrous septa, which corresponded to the appearance of various signal characteristics on T1-weighted and T2-weighted MR images. Fibrous septa also corresponded to areas of peripheral enhancement on contrast-enhanced MR images. Heterogeneous enhancement on contrast-enhanced MR images also correlated with the presence of intratumoral cysts (n=4) and hemorrhage (n=1). These areas corresponded to areas of high signal intensity on T2-weighted MR images. Geographic areas of necrosis were present in five patients (26%). Lobules often showed higher cellularity at the periphery, which corresponded to peripheral or diffuse enhancement on contrast-enhanced MR images. Hyaline cartilage had developed in one patient, although there were small islands of immature cartilage in several patients. All tumors were characterized microscopically by cords or clusters of neoplastic cells, which demonstrated a modest amount of eosinophilic, granular-to-vacuolated cytoplasm and uniform ovoid nuclei. Fourteen tumors were assigned grade 1 malignancy, and the remaining six tumors were grade 2.

All patients underwent surgical resection as a primary therapy. Surgical margins were adequate in 11 patients and inadequate in four. All patients with inadequate surgical margins had undergone subsequent wide resection. Chemotherapy (carboplatinum 1,000 mg, Adriamycin 60 mg) and radiotherapy (50 Gy) were included in the treatment regimen of one patient. The median follow-up period of all cases was 61 months. There were local recurrences in three patients (16%) at a median interval of 12 months. Metastases occurred in three cases (16%). The sites of metastases were lungs (n=3) followed by bone (n=1). Two patients that were being followed-up had died from the disease; 17 patients were alive with the disease or with no evidence of disease.

Discussion

EMC has been described as a rare, adult, soft-tissue sarcoma. It commonly affects patients aged 50–60 years but is also known to occur in younger people [1, 2]. Patients usually present with non-specific symptoms, including tenderness and palpable mass [1–4]. Patient demographics and clinical symptoms in our series were similar to those in previous studies [1, 2].

Unlike in the previous reports [12–14], signal characteristics on T1-weighted MR images were varied. In our study, tumors showed predominantly low (5%), intermediate (80%), or high (15%) signal intensity relative to muscle on T1-weighted MR images. These features on T1-

weighted MR images might be due to underlying pathologic changes. In all our cases, myxoid and gelatinous nodules, separated by fibrous septa, were frequently apparent on pathologic observation. Pathologically, EMC often consists of hemorrhagic changes [2]. MRI evidence of hemorrhagic foci of high signal intensity on T1-weighted image was seen in one of our patients. Although this was in accordance with pathologic findings, the occurrence of hemorrhage was not a common finding on MR images.

A few case series have demonstrated homogeneous or heterogeneous enhancement on contrast-enhanced MR images [12–14]. In fact, all our cases showed heterogeneous enhancement. Peripheral enhancement was also found in 32% of our cases after administration of contrast material at MRI. These results suggest that the enhancement pattern on MR images may depend on tumor heterogeneity in EMC. The high frequency of peripheral enhancement that was demonstrated on contrast-enhanced T1-weighted MR images was in good accordance with the gross pathologic features.

High signal intensity on T1- weighted images corresponded to areas of hemorrhage identified pathologically, as described in our study. Although intratumoral hemorrhage was found in only one case, hemorrhagic soft-tissue sarcoma could be considered in the differential diagnosis. Synovial sarcoma is often associated with hemorrhagic change, representing various MR signal patterns. Triple-signal pattern, one of the heterogeneous patterns on T2-weighted MR images, is considered to be not specific but suggestive of the diagnosis, given the most prevalent age [15]. Fluid–fluid levels may occur whenever substances of differing densities are contained within a cystic or compartmentalized structure. The levels are depicted when imaging is performed in a gravity-dependent plane. The presence of fluid–fluid levels in soft-tissue tumors cannot be considered diagnostic of any particular tumor, including synovial sarcoma and malignant fibrous histiocytoma [16]. A sign of fluid–fluid level was seen in none of our cases on T2-weighted MR images, which would suggest that this finding might be less frequent in patients with EMC.

The identification of the highly specific balanced chromosomal rearrangement in EMC provides a valuable tool for diagnosis at the molecular level. In our series, 68% of tumors consisted of three variant fusions. The relationship between cytogenetic variants and imaging findings were not fully understood. Although signal characteristics on T1-weighted and T2-weighted MR images were non-specific, peripheral enhancement on contrast-enhanced MR images was seen more frequently in tumors with the EWS-CHN variant than in those with other cytogenetic variants, according to our results. Peripheral enhancement on contrast-enhanced MR images may be characteristic for this entity, because most patients with EMC have chromosomal aberration of EWS-CHN [6–11].

The imaging features of EMC reflect the underlying pathologic findings [12–14]. Extracompartmental extension and cortical destruction, with soft-tissue mass, were found in 26% of cases, according to our results. In addition, all tumors with TAF2N-CHN or TFG-TCH variants showed invasion of extracompartmental structure, bone, or vessels. Although the association between imaging findings and cytogenetic variants is obscure, the invasive nature of MRI findings may be characteristic in these variants.

As with other soft -tissue sarcomas in adults, surgical resection is recommended in EMC. EMC typically has a prolonged clinical course with complete resection [4]. However, the behavior of EMC has been reported to be poor, with frequent local recurrences and distant metastases [1, 3]. Sixteen percent of our patients developed local recurrences, and metastases occurred in 16% of our cases. EMC seems to have frequent recurrences and metastases, and long-term follow-up is needed.

We recognize certain limitations of our study. Because of the referral basis of our cases, we were unable to control the MRI parameters. However, our retrospective review includes a greater number of cross-sectional imaging studies than does any previous study [5–8]. Despite these limitations, our study may add substantial understanding of imaging features of EMC.

Conclusion

Characteristic imaging features of EMC are multi-nodular soft-tissue masses, presenting predominantly hyper-signal intensity on T2-weighted MR images and heterogeneous enhancement after administration of contrast material. Peripheral enhancement was seen more frequently in tumors with the EWS-CHN variant than in those with other cytogenetic variants. Tumors with TAF2N-CHN or TFG-TCH variants showed invasion of extracompartmental structure, bone, or vessels. These features clearly reflect the underlying histopathologic characteristics of EMC.

References

1. Saleh G, Evans HL, Ro JY, Ayala AG. Extraskeletal myxoid chondrosarcoma. A clinicopathologic study of ten patients with long-term follow-up. Cancer 1992;15 70:2827–30
2. Meis-Kindblom JM, Bergh P, Gunterberg B, Kindblom LG. Extraskeletal myxoid chondrosarcoma: a reappraisal of its morphologic spectrum and prognostic factors based on 117 cases. Am J Surg Pathol 1999;23:636–50
3. Lucas DR, Fletcher CD, Adsay NV, Zalupski MM. High-grade extraskeletal myxoid chondrosarcoma: a high-grade epithelioid malignancy. Histopathology 1999;35:201–8

Jpn J Clin Oncol 2005;35(8)444–452
doi:10.1093/jjco/hyi128

Incidence of Multiple Primary Malignancies in a Cohort of Adult Patients with Soft Tissue Sarcoma

Ukihide Tateishi[1], Tadashi Hasegawa[2], Seiichiro Yamamoto[3], Umio Yamaguchi[4], Ryohei Yokoyama[5], Hiroshi Kawamoto[3], Mitsuo Satake[1] and Yasuaki Arai[1]

[1]Diagnostic Radiology Division, [2]Pathology Division and [4]Orthopedic Surgery Division, National Cancer Center Hospital and Institute, [3]Statistics and Cancer Control Division, Research Center for Cancer Prevention and Screening, National Cancer Center, Tokyo and [5]Department of Orthopedic Surgery, Kyushu Cancer Center, Fukuoka, Japan

Received March 6, 2005; accepted June 1, 2005; published online July 15, 2005

Objective: Some studies to date have suggested the development of multiple primary malignancies in patients with soft tissue sarcoma. The current study was performed to quantify the risk of development of multiple primary malignancies in adult patients with soft tissue sarcoma.
Methods: A total of 406 consecutive patients who were diagnosed with soft tissue sarcoma were identified in the study analysis. The cumulative incidence of multiple malignancies was calculated by comparing Kaplan–Meier curves and log-rank tests from each histological type. A Cox proportional hazards model was used to estimate the influence on the hazard ratio (HR) of each variable.
Results: A total of 35 patients with soft tissue sarcoma (9%), having preceding ($n = 15$) and subsequent ($n = 20$) malignancies other than soft tissue sarcoma were documented. The 5- and 10-year estimated cumulative incidence of multiple primary malignancies were 7.6 and 12.3%, respectively. The hazard risk of multiple primary malignancies adjusted for potential confounding variables was significantly associated with age at diagnosis (HR = 1.51, $P = 0.0019$). The risk of multiple primary malignancies was also increased in patients with myxofibrosarcoma adjusted by the potential confounding variables (HR = 2.34, $P = 0.048$). The 5- and 10-year estimated cumulative incidence of multiple primary malignancies in patients with myxofibrosarcoma were both 16.9%.
Conclusion: The results of our study confirm that the risk of multiple malignancies appears to be impacted by age at the time of diagnosis of the first tumor and by the histological type of myxofibrosarcoma.

Key words: soft tissue sarcoma – myxofibrosarcoma – multiple malignancies – second primary tumor

INTRODUCTION

The development of multiple malignancies in a single individual has been reported after successful treatment of primary tumors (1,2). The greatest attention has been focused on second primary tumors (SPTs) after treatment of malignant lymphoma (3), retinoblastoma (4) and malignant germ cell tumor (5,6) because good cure rates have been achieved for many years, resulting in many long-term survivors.

The occurrence of multiple malignancies in patients with soft tissue sarcoma (STS) has also been reported (7,8). Studies focused on patients with osteosarcoma have revealed an overall 10-year cumulative incidence of SPT of 2.0–3.1% (9,10). Adult patients with STS have been found to develop other malignant neoplasms either before or after the diagnosis of STS, and this phenomenon occurred at a significantly higher rate than reported for the occurrence of STS in the general cancer population (11).

However, the risk of SPT after treatment of the first tumor has been mainly described in children with STS. Although we have observed the occurrence of multiple primary malignancies that occurred in adult patients with various histological types of STS, especially pleomorphic malignant fibrous histiocytoma (MFH) and myxofibrosarcoma, in daily clinical practice there has been little information on the management of these patients. The current study was therefore undertaken to assess the risk of development of another primary malignant tumor in adult patients with STS.

MATERIALS AND METHODS

PATIENTS

The records of 500 consecutive adult STS patients diagnosed and treated between February 1962 and August 2003 were

For reprints and all correspondence: Ukihide Tateishi, Division of Diagnostic Radiology, National Cancer Center Hospital, 5-1-1, Tsukiji, Chuo-ku, 104-0045 Tokyo, Japan. E-mail: utateish@ncc.go.jp

retrieved from the pathology files of our institution. This study was approved by the local Ethics Committees after confirmation of informed consent by the patients to a review of their records and images. The enrollment criteria consisted of (i) adult STS patients whose pathological specimens and medical charts were available for review; and (ii) patients who were not lost to follow-up. The exclusion criteria consisted of (i) subjects whose pathological specimens and medical charts were insufficient for review; and (ii) subjects whose pathological subtypes were considered to be rare in the clinical setting. Thus, 94 patients (19%) whose tumors comprised epithelioid sarcoma (n = 25), alveolar soft part sarcoma (n = 20), clear cell sarcoma (n = 16), extraskeletal myxoid chondrosarcoma (n = 20) or extraskeletal osteosarcoma (n = 13) were excluded from the analysis, and the 406 patients with common STSs were included in the analysis. The patients consisted of 223 men and 183 women, and they ranged in age from 16 to 87 years (median age: 53 years). During the period 1962–2003, the concept of MFH or myxofibrosarcoma changed. Twenty-three myxofibrosarcomas (34%) which were previously diagnosed as myxoid variant of MFH or solely fibrosarcoma were reclassified by the review of pathological examinations. Autopsy was performed in 16 cases (4%) and their pathological specimens were also available for review.

In the patients who developed multiple primary malignancies, we investigated: age at diagnosis, gender, family history, anatomic site, tumor size, depth, surgical margin, histological type, MIB-1 score, grade, whether chemotherapy has been performed, whether radiation therapy has been performed and the outcome. If the patient had died, the date and the cause of death were also noted.

Patients were followed-up with regard to survival until August 31, 2004, at which time 250 patients were alive with no evidence of disease, 26 patients were alive with disease and 130 patients had died of their disease. The malignancy-free survival period (MFSP) was measured from the date of diagnosis of STS to the date of the first observations of multiple malignancies. If the detection of malignancy other than STS preceded the date of diagnosis of the STS, the MFSP was recorded as 0. If a patient was alive without developing any multiple malignancies at the last visit, the data on MFSP were censored as of the date when the survival was confirmed. If a patient died without detection of other primary malignancies, the MFSP was censored at the date of death. If other primary malignancy was found at autopsy, the date of death was treated as an event.

Histological slides of the primary tumors of all patients were reviewed for diagnosis by two experts. Whenever necessary, immunohistochemistry was used to confirm the diagnosis or tumor type according to the WHO classification (12). MIB-1 immunostaining was performed to grade all tumors. An MIB-1 score of 1 was assigned to lesions with an MIB-1 labeling index (LI) of 0–9%, an MIB-1 score of 2 was given to lesions with an MIB-1 LI of 10–29%, and an MIB-1 score of 3 was given to lesions with an MIB-1 LI $\geq$ 30%. There were tumors with an MIB-1 score of 1 (n = 140; 35%), 2 (n = 62; 15%) and 3 (n = 204; 50%). The histological grade is a three-grade system obtained by adding the scores for tumor differentiation, tumor necrosis and MIB-1 score, each of which was given a score of 0–3 (13). By using the grading system, tumors corresponded to grade 1 (n = 128; 32%), grade 2 (n = 107; 26%) and grade 3 (n = 171; 42%), respectively. Tumor depth was measured relative to muscular fascia that had been invaded and was characterized as superficial or deep. The vast majority of lesions (n = 322; 79%) were deep seated, and 94 tumors were superficial.

Statistical Analysis

Univariate analysis of the cumulative incidence of multiple malignancies was performed by comparing Kaplan–Meier curves and log-rank tests from each histological type. The hazard ratio (HR) of each variable was estimated by using a Cox proportional hazards model in the univariate and multivariate analyses. The following factors are considered as potential confounding factors for the incidence of multiple malignancies: age at presentation, gender, family history of malignant neoplasm, anatomic site, tumor size, depth, surgical margin, histological type, MIB-1 score (1, 2 or 3) and grade (1, 2 or 3). Variable selection by the backward elimination (α = 0.2) procedure was performed in the multivariate analyses. All analyses were performed with SAS Software (version 6.12; SAS Institute, Cary, NC).

RESULTS

Tumors had a diameter >5 cm in 302 patients (74%). Most tumors were located in the extremities (n = 244; 60%) compared with the trunk (n = 96; 24%) and other sites (n = 66; 16%). The histological types consisted of liposarcoma (n = 159; 39%), myxofibrosarcoma (n = 67; 17%), pleomorphic MFH (n = 53; 13%), synovial sarcoma (n = 50; 12%), leiomyosarcoma (n = 32; 8%), malignant peripheral nerve sheath tumor (MPNST; n = 25; 6%) and fibrosarcoma (n = 20; 4%). Of these 406 tumors, 371 tumors (91%) did not develop multiple malignancies (Table 1).

A total of 35 patients (9%) with STS were documented in the study population, among whom the STS was preceded by (n = 15) and followed by (n = 20) malignancies other than STS. The median age at the time of diagnosis of the first tumors was 63 years (range 39–79 years). The SPTs were diagnosed a median of 64 months after the diagnosis of the first tumor. A third primary tumor (TPT) was found in eight patients, a median of 127 months after the first tumor. One patient was found to have a fourth primary tumor 331 months after the first tumor. The overall 5- and 10-year estimated cumulative incidence of multiple primary malignancy was 7.6% [95% confidence interval (CI) 4.7–10.4] and 12.3% (95% CI 7.4–18.0), respectively.

Information related to the patients is listed in Table 2. The most frequent histological types of STS were myxofibrosarcoma (n = 13; 19.4%) and pleomorphic MFH (n = 6; 11.3%).

Table 1. Demographics of patients without multiple malignancies

Variables	LS	MFS	PMFH	SS	LMS	MPNST	FS	Total
n	148	54	47	50	30	24	18	371
Mean age (years)	51.6	60.5	57.9	32.9	55.3	50.0	42.4	50.9
SD	12.8	13.1	14.3	15.4	13.8	15.5	21.5	16.3
Range	18–87	29–87	26–86	18–72	30–83	28–74	18–87	18–87
Gender								
Male	89	27	31	22	11	9	12	201
Female	59	27	16	28	19	15	6	170
Distribution								
Extremities	91 (62)	37 (69)	31 (66)	36 (72)	6 (20)	13 (54)	12 (67)	226 (60)
Trunk	21 (14)	16 (30)	15 (32)	11 (22)	9 (30)	10 (42)	5 (28)	87 (23)
Others	36 (24)	1 (2)	1 (2)	3 (6)	15 (50)	1 (4)	1 (6)	58 (15)
MIB-1 score								
1	99 (67)	10 (19)	2 (4)	5 (10)	2 (7)	5 (21)	7 (39)	130 (34)
2	17 (12)	14 (26)	3 (6)	12 (24)	3 (10)	1 (4)	6 (33)	56 (15)
3	32 (22)	30 (56)	42 (89)	33 (66)	25 (83)	18 (75)	5 (29)	185 (49)
Grade								
1	94 (64)	9 (17)	2 (4)	0	2 (7)	4 (17)	8 (44)	119 (31)
2	22 (15)	34 (63)	8 (17)	14 (28)	7 (23)	2 (8)	7 (39)	94 (25)
3	32 (22)	11 (20)	37 (79)	36 (72)	21 (70)	18 (75)	3 (17)	158 (42)
Depth								
Superficial	19 (13)	16 (30)	14 (30)	7 (14)	6 (20)	4 (17)	5 (28)	71 (19)
Deep	129 (87)	38 (70)	33 (70)	43 (86)	24 (80)	20 (83)	13 (72)	300 (79)
Size (cm)								
0–5	10 (7)	20 (37)	15 (32)	24 (48)	8 (27)	7 (29)	11 (61)	95 (26)
5–10	59 (40)	25 (46)	17 (36)	18 (36)	13 (43)	13 (54)	5 (28)	150 (40)
>10	79 (53)	9 (17)	15 (32)	8 (16)	9 (30)	4 (17)	2 (11)	126 (33)
Margin								
Adequate	105 (71)	46 (85)	44 (94)	45 (90)	26 (87)	17 (71)	15 (83)	298 (79)
Inadequate	43 (29)	8 (15)	3 (6)	5 (10)	4 (13)	7 (29)	3 (17)	73 (19)
Chemotherapy	28 (19)	13 (24)	24 (51)	31 (62)	12 (40)	13 (54)	6 (33)	127 (34)
Radiation therapy	36 (24)	19 (35)	14 (30)	11 (22)	10 (33)	10 (42)	4 (22)	104 (27)
Family history of cancer	21 (49)	4 (9)	6 (14)	2 (5)	2 (5)	6 (14)	2 (5)	43 (12)
Survival rate (%)								
5 year	86.7	89.3	51.6	61.8	27.5	45.2	66.2	71.7
10 year	78.5	69.6	41.4	48.4	27.5	24.1	48.4	57.7

The numbers in parentheses are percentages.
LS, liposarcoma; MFS, myxofibrosarcoma; PMFH, pleomorphic malignant histiocytoma; SS, synovial sarcoma; LMS, leiomyosarcoma; MPNST, malignant peripheral nerve sheath tumor; FS, fibrosarcoma.

Less common histological types consisted of fibrosarcoma ($n = 2$; 10%), liposarcoma ($n = 11$; 6.9%), leiomyosarcoma ($n = 2$; 6.3%) and MPNST ($n = 1$; 4%).

The risk of multiple malignancies differed significantly according to the histological type of the STS (log rank test: $P = 0.0055$). None of the patients with synovial sarcoma had multiple malignancies. The multivariate analysis adjusted for potential confounding variables showed a higher risk of multiple malignancy in patients with myxofibrosarcoma (Table 3). When patients with pleomorphic MFH and myxofibrosarcoma were combined into the same histological category, the risk of multiple malignancies was 2.13 (95% CI 1.00–4.55, $P = 0.0496$). However, no significant association was found between risk of multiple malignancies and survival rate, or familiar history of malignant neoplasm in pleomorphic MFH and myxofibrosarcoma.

Table 2. Demographics of patients with multiple malignancies

Variables	MFS	PMFH	Other tumors	Total
n	13 (37)	6 (17)	16 (46)	35
Mean age (years)	63.8	66.5	58.8	62.0
SD	11.4	13.1	10.9	11.5
Range	45–79	47–76	39–79	39–79
Gender				
Male	10	5	7	22
Female	3	1	9	13
Distribution				
Extremities	10 (77)	2 (33)	6 (38)	18 (51)
Trunk	3 (23)	4 (66)	2 (13)	9 (26)
Others	0	0	8 (50)	8 (23)
MIB-1 score				
1	3 (23)	0	7 (44)	10 (29)
2	3 (23)	0	3 (19)	6 (17)
3	7 (54)	6 (100)	6 (38)	19 (54)
Grade				
1	3 (23)	0	6 (38)	9 (26)
2	8 (62)	1 (17)	4 (26)	13 (37)
3	2 (15)	5 (83)	6 (38)	13 (37)
Depth				
Superficial	9 (69)	4 (66)	0	13 (37)
Deep	4 (30)	2 (33)	16 (100)	22 (63)
Size (cm)				
0–5	5 (38)	1 (17)	3 (19)	9 (26)
5–10	7 (54)	5 (83)	4 (26)	16 (46)
10+	1 (8)	0	9 (69)	10 (29)
Margin				
Adequate	11 (85)	6 (100)	11 (69)	28 (80)
Inadequate	2 (15)	0	5 (31)	7 (20)
Survival rate (%)				
5 year	84.6	50.0	66.1	70.0
10 year	70.5	16.7	27.3	43.1

The numbers in parentheses are percentages.
MFS, myxofibrosarcoma; PMFH, pleomorphic malignant fibrous histiocytoma.

Twelve patients (37.1%) had a family history of cancer. One patient had familial adenomatous polyposis (FAP) with a germline mutation in the APC gene. Two patients with a second or third primary STS had previously received systemic chemotherapy and radiation therapy. Patients with a second or third primary cancer whose STS preceded it had previously received chemotherapy ($n = 3$) and radiation therapy ($n = 4$). Only one patient had a third primary cancer within the radiation field.

Age at the time of diagnosis was associated with increased risk of multiple malignancies in the unadjusted analysis (HR = 1.52, 95% CI 1.17–1.97, $P = 0.0016$), but no significant association was found with gender, family history of cancer, MIB-1 score, grade, tumor size, depth or margin. Furthermore, no interaction was evidenced between the risk of multiple malignancies and having received chemotherapy or radiation therapy.

Table 3. Hazard risk of multiple malignancies adjusted for potential confounding variables

Variables	HR	95% CI	*P*-value
Age	1.51	1.17–1.96	0.0019
Tumor size	1.03	0.99–1.07	0.18
MFS	2.34	1.01–5.41	0.048
PMFH	1.85	0.69–4.97	0.22
Other tumors*	1	–	–

*Adjusted hazard risk (HR) referenced to other tumors is presented.
MFS, myxofibrosarcoma; PMFH, pleomorphic malignant fibrous histiocytoma.

Myxofibrosarcoma developed as the first tumor in three patients, the second tumor in seven, the third tumor in two, and the fourth tumor in one (Table 4). The MFSP between the diagnosis of the first and second malignancies ranged from 4 to 275 months (median: 69.0 months). The TPTs were detected within 142 months after the diagnosis of the first tumor. One myxofibrosarcoma of the thigh developed after radiation therapy for a second primary esophageal carcinoma. The fourth primary tumor developed in a patient who had undergone surgical resection three times for carcinomas of the colon and cecum. The patient developed a myxofibrosarcoma of the thigh that was treated by surgery and chemotherapy 120 months after the diagnosis of the SPT. The 5- and 10-year estimated cumulative incidence of multiple malignancies in patients with myxofibrosarcoma were both 16.9% (95% CI 7.8–26.1; Fig. 1). The overall survival time of the 13 patients in the group after the diagnosis of the first tumor ranged from 10 to 408 months (median: 148.0 months). The 5-year survival rate of the group was similar to that of the patients without multiple malignancies (84.6 versus 89.3%, $P = 0.81$).

Pleomorphic MFH occurred as the first tumor in five patients (Table 5), and in one patient it was followed by esophageal carcinoma. The MFSP between the diagnosis of the first and second malignancies varied from 17 to 94 months (median: 74.0 months). The 5-year estimated cumulative incidence of multiple malignancies in patients with pleomorphic MFH was 10.2% (95% CI 0.0–20.6; Fig. 1). The overall survival time of the six patients in this group ranged from 48 to 155 months (median: 113.0 months), and the 5-year survival rate was not significantly different from that of pleomorphic MFH patients without multiple malignancies (50.0 versus 51.6%, $P = 0.32$). One patient died of the first tumor after developing a metastasis, and the other five patients died of the SPT.

Nineteen multiple malignancies were associated with four types of adult STSs: liposarcomas in 11 patients, fibrosarcomas in two, leiomyosarcomas in two and MPNST in one (Table 6). The MFSP between the diagnosis of the primary malignancy

Table 4. Myxofibrosarcoma with multiple malignancies (n = 13)

Patient	Age (years)	Gender	FT	Site	CT	RT	MFSP	SPT	Site	CT	RT	MFSP from SPT	TPT	Site	CT	RT	MFSP from TPT	FPT	Site	CT	RT	Prognosis	OS
1	55	Male	MFS	Thigh	–	–	4	Ad	Stomach	–	–	–	–	–	–	–	–	–	–	–	–	NED	10
2	68	Male	MFS	Buttock	–	–	8	Sq	Pharynx	–	50 Gy	–	–	–	–	–	–	–	–	–	–	DOD	246
3	48	Female	MFS	Leg	–	–	130	Ad	Ovary	CDDP + ADR + CPA CDDP + Taxel	–	–	–	–	–	–	–	–	–	–	–	DOD	177
4	69	Male	Ad	Stomach	–	–	38	MFS	Thigh	–	–	–	–	–	–	–	–	–	–	–	–	DOD	101
5	66	Male	TCC	Bladder	–	–	11	MFS	Chest wall	–	–	5	TCC	Bladder	ADR	–	–	–	–	–	–	NED	156
6	69	Male	Sq	tongue	CDDP 5FU	50 Gy	84	MFS	Leg	–	–	7	Sq	Gingiva	–	–	–	–	–	–	–	NED	91
7	70	Male	Ad	Rectum	–	–	19	MFS	Arm	–	42 Gy	–	–	–	–	–	–	–	–	–	–	DOD	34
8	74	Male	Ad	Prostate	–	–	4	MFS	Arm	–	–	–	–	–	–	–	–	–	–	–	–	NED	24
9	48	Female	Ad	Breast	–	–	85	MFS	Arm	–	–	–	–	–	–	–	–	–	–	–	–	NED	143
10	79	Female	RCC	Kidney	–	–	139	MFS	Arm	–	–	–	–	–	–	–	–	–	–	–	–	NED	148
11	77	Male	Ad	Colon*	–	–	275	Ad	Stomach	–	–	105	MFS	Leg	–	–	–	–	–	–	–	NED	381
12	45	Male	Ad	Stomach	–	–	216	Sq	Esophagus	–	60 Gy	84	MFS	Thigh	–	–	–	–	–	–	–	NED	408
13	62	Male	Ad	Colon	–	–	69	Ad	Cecum	–	–	142	Ad	Colon	–	–	120	MFS	Thigh	CDDP	–	NED	331

FT, first tumor; CT, chemotherapy; RT, radiotherapy; MFSP, malignancy-free survival period (months); SPT, second primary tumor; TPT, third primary tumor; FPT, fourth primary tumor; DOD, died of disease; NED, no evidence of disease; OS, overall survival (months); MFS, myxofibrosarcoma; Ad, adenocarcinoma; Sq, squamous cell carcioma; TCC, transitional cell carcinoma; RCC, renal cell carcinoma; CDDP, cisplatin; ADR, adriamycin; CPA, cyclophosphamide; 5FU, 5-fluorouracil.
*Synchronous tumor.

and the second malignancy ranged from 1 to 141 months (median: 60.0 months). The 5- and 10-year estimated cumulative incidence of multiple malignancies in this group was 5.1% (95% CI 2.2–8.0) and 9.7% (95% CI 3.8–15.7%; Fig. 1), respectively. The overall survival time of the 16 patients from the time of diagnosis of the first tumor ranged from 6 to 223 months (median: 96.5 months). No significant difference in 5-year survival rate was found between the patients with and without multiple malignancies (66.1 versus 71.6%, $P = 0.80$).

DISCUSSION

The objective of this study was to review the incidence of multiple malignancy in adult STS patients. The results of the analysis showed that 9% of the patients had multiple malignancies. The 5- and 10-year estimated cumulative incidence of multiple malignancy was 7.6% (95% CI 4.7–10.4) and 12.3% (95% CI 7.4–18.0), respectively. In addition, the risk of multiple malignancy appeared to be impacted by age at the time of diagnosis of the first tumor and by the histological type of myxofibrosarcoma.

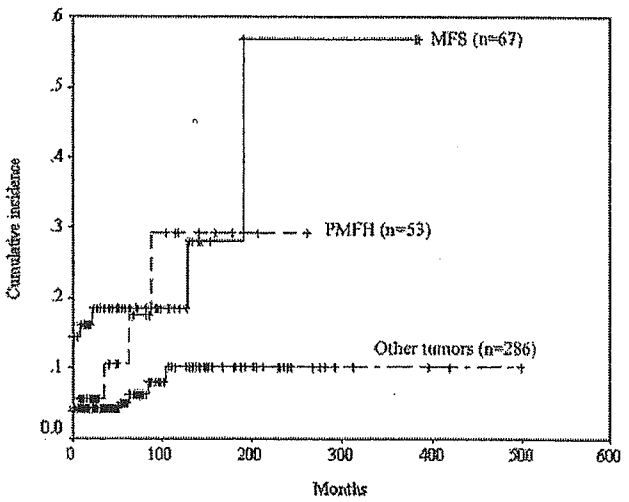

Figure 1. Cumulative incidence of multiple malignancies in STS. MFS, myxofibrosarcoma; PMFH, pleomorphic malignant fibrous histiocytoma. A statistically significant difference is found between the three groups (log rank $P = 0.002$).

The results of this analysis add to the evidence of an association between STS and the risk of multiple malignancy. The results are consistent with the findings in the cohort study Merimsky et al. that assessed the risk of multiple malignancies associated with STS (11). In their study, 28 of 375 adult patients (7.5%) with STS were found to have developed another primary malignant neoplasm either before or after the diagnosis of STS, a significantly higher rate than reported for the occurrence of STS in the general cancer patient population (1.0%). In addition, they also observed an association between primary MFH and the occurrence of renal cell carcinoma. However, Merimsky et al. did not evaluate risk according to histological types of STS, and they included several patients with bone sarcoma in their analysis. Thus, our study expanded on the findings of Merimsky et al. by assessing the impact of histological type.

Previous studies in patients with STS have found frequencies of an SPT ranging from 1.2 to 6.0% (14,15). In contrast, one study that investigated the risk of developing SPT in patients with non-Hodgkin lymphoma yielded a frequency of 15.4% (16). However, the populations in these studies were mainly children or adolescents. In our study, the rate of association of an SPT or TPT with STS was 9.0%, suggesting that the frequency of multiple malignancies is similar in the different age populations. Age at the time of diagnosis was strongly associated with increased risk of multiple malignancies in adult patients with STS.

The results of our study showed that the risk of multiple malignancies was similar when the analysis was conducted separately for patients with pleomorphic MFH and myxofibrosarcoma, the most common types of STS. Multiple malignancies were detected in six patients with pleomorphic MFH, and in five patients where the pleomorphic MFH was preceded by another malignant tumor. Similarly, the other malignancy was detected first in three of the 13 patients (23%) with myxofibrosarcoma and subsequently in the other

Table 5. Pleomorphic MFH with multiple malignancies ($n = 6$)

Patient	Age (years)	Gender	FT	Site	CT	RT	MFSP	SPT	Site	CT	RT	MFSP from SPT	TPT	Site	CT	RT	Prognosis	OS
1	76	Male	PMFH	Shoulder	–	32.5 Gy	64	Ad	Bile duct	MMC	–	–	–	–	–	–	DOD	78
2	76	Male	PMFH	Thigh	–	–	84	Ad	Lung	–	–	–	–	–	–	–	DOD	155
3	53	Male	PMFH	Elbow	VCR ADR	–	6	Sq	Tongue	–	–	–	–	–	–	–	DOD	106
4	47	Male	PMFH	Buttock	–	–	31	Ad	Colon	–	–	–	–	–	–	–	DOD	48
5	76	Male	PMFH	Back	–	50 Gy	121	Ad	Stomach	–	50 Gy	–	–	–	–	–	DOD	138
6	71	Male	Sq	Esophagus	–	–	94	PMFH	Back	–	–	7	Ad	Stomach	–	–	DOD	120

FT, first tumor; CT, chemotherapy; RT, radiotherapy; MFSP, malignancy-free survival period (months); SPT, second primary tumor; TPT, third primary tumor; DOD, died of disease; NED, no evidence of disease; OS, overall survival (months); PMFH, pleomorphic malignant fibrous histiocytoma; Sq, squamous cell carcioma; Ad, adenocarcinoma; VCR, vincristine; ADR, adriamycin; MMC, mitomycin C.

Table 6. Other tumors with multiple malignancies (n = 16)

Patient	Age (years)	Gender	FT	Site	CT	RT	MFSP	SPT	Site	CT	RT	MFSP from SPT	TPT	Site	CT	RT	Prognosis	OS
1	62	Female	FS	Thigh	–	–	1	Ad	Uterine	–	–	–	–	–	–	–	DOD	6
2	57	Female	LS (D)	Retroperitoneum	–	40 Gy	29	Ad	Breast	–	–	–	–	–	–	–	DOD	108
3	42	Female	LS (D)	Retroperitoneum	ADR VCR	–	75	Pap	Thyroid	NA	NA	–	–	–	–	–	DOD	78
4	57	Male	LS (M)	Thigh	VCR	–	141	Sq	Larynx	–	60 Gy	–	–	–	–	–	NED	223
5	59	Male	LS (M)	Thigh	–	–	4	Ad	Lung*	–	–	–	–	–	–	–	NED	38
6	61	Male	LS (WD)	Retroperitoneum	–	–	81	Ad	Prostate	SR	62 Gy	–	–	–	–	–	NED	85
7	63	Male	LS (WD)	Retroperitoneum	–	–	8	Ad	Prostate	LA	–	–	–	–	–	–	NED	9
8	70	Female	Ad	Breast	–	–	60	FS	Chest wall	–	–	17	Ad	Stomach	–	–	NED	112
9	60	Male	DLBL	Thyroid	CHOP	–	81	L	Leg	–	–	–	–	–	–	–	NED	117
10	39	Female	Ad	Breast	–	–	60	L	Buttock	CPA, VCR, ADM, DTIC	–	–	–	–	–	–	DOD	212
11	50	Female	Ad	Breast	–	–	105	LS (M)	Thigh	–	50 Gy	–	–	–	–	–	DOD	127
12	64	Male	Ad	Rectum	–	–	50	LS (M)	Leg	–	–	–	–	–	–	–	DOD	61
13	43	Female	Ad	Breast	–	–	102	LS (WD)	Retroperitoneum	–	–	–	–	–	–	–	NED	121
14	63	Female	Ad	Breast	–	–	29	LS (WD)	Retroperitoneum	–	–	–	–	–	–	–	NED	75
15	71	Female	Pap	Thyroid	–	–	2	MPNST	Retroperitoneum	–	–	–	–	–	–	–	NED	15
16	79	Male	TCC	Bladder	–	–	106	Ad	Lung	–	–	12	LS (D)	Retroperitoneum	–	–	DOD	146

FT, first tumor; CT, chemotherapy; RT, radiotherapy; MFSP, malignancy-free survival period (months); SPT, second primary tumor; TPT, third primary tumor; DOD, died of disease; NED, no evidence of disease; OS, overall survival (months); FS, fibrosarcoma; Ad, adenocarcinoma; LS (D), liposarcoma (dedifferentiated); Pap, papillary carcinoma; LS (M), liposarcoma (myxoid); Sq, squamous cell carcinoma; LS (WD), liposarcoma (well differentiated); DLBL, diffuse large B-cell lymphoma; MPNST, malignant peripheral nerve sheath tumor; TCC, transitional cell carcinoma; CHOP, cyclophosphamide, adriamycin, vincristine, prednisolone; ADR, adriamycin; VCR, vincristine; CPA, cyclophosphamide; DTIC, dacarbazine; SR, zoladex; LA, leuplin; NA, not applicable.
*Synchronous tumor.

10 patients (77%). Some investigators consider a pleomorphic MFH to be a high grade tumor that has a substantially high metastatic rate and poor prognosis (17,18). Myxofibrosarcoma is a distinct fibroblastic neoplasm that may recur and has a relatively poor prognosis (19–21). In our study, univariate analysis revealed that no significant association was found between risk of multiple malignancy and survival rate, or familiar history in pleomorphic MFH and myxofibrosarcoma.

A family history of cancer and genetic predisposition to cancer may be associated with a risk of multiple malignancies. A correlation between the incidence of multiple malignancy and familial aggregation has been demonstrated in Li–Fraumeni syndrome (22). Similarly, genetic factors have an impact on the risk of various histological types of SPT (23,24). It was not likely that these factors would profoundly influence the risk related to development of multiple malignancies since there was no significant association between familial history of cancer and the risk of multiple malignancies in our study. Some rare familial syndromes are associated with an excess risk of multiple malignancies. There was a patient with FAP with a germline mutation of the APC gene. This patient developed myxofibrosarcoma of the thigh as a fourth primary tumor after surgical treatment of colon cancers three times.

Despite the fact that the known carcinogenic effects of chemotherapy and radiation therapy are associated with an increased risk of developing SPT (25,26), no interaction was found with having received chemotherapy and radiation therapy according to the results of the multivariate analysis. The lack of agreement between our findings and those of other investigators may be attributable to the small number of patients treated by chemotherapy and radiation therapy: only two patients with second or third primary STS were previously treated by chemotherapy and radiation therapy.

Our results showed that multiple malignancies occurred in 9% of patients with STS, and that the rate of occurrence depended on the histological type. The 5-year survival rate of patients with multiple malignancies according to the histological type of STS was not statistically different from that of the patients without multiple malignancies. Many histological types of multiple malignancies occurred in various organs, suggesting that the whole-body screening to detect other primary malignant neoplasms in addition to local recurrence or distant metastasis should be considered in the management of patients with multiple primary malignancies. Recent prospective studies have highlighted the potential diagnostic role of whole-body [^{18}F]fluorodeoxyglucose positron emission tomography (FDG PET) for evaluation of malignant tumors. FDG PET is an accurate non-invasive test for diagnosis of adult STS and has high sensitivity and intermediate specificity for malignancy. We recommend a whole-body FDG PET scan in the search for a second malignancy in patients with multiple primary malignancies.

In summary, the results of our study confirm the incidence of multiple primary malignancies in adult patients with STS, and the histological type of myxofibrosarcoma was found to be associated with an increased risk of multiple primary malignancy. Physicians should be aware of the increased risk of multiple primary malignancies in patients with myxofibrosarcoma, and whole-body screening to detect other malignant neoplasms is desirable.

References

1. Evans HS, Lewis CM, Robinson D, Bell CMJ, Høller H, Hodgson SV. Incidence of multiple primary cancers in a cohort of women diagnosed with breast cancer in southeast England. *Br J Cancer* 2001;84:435–40.
2. Rubino C, de Vathaire F, Dottorini ME, Hall P, Schvartz C, Couette JE, et al. Second primary malignancies in thyroid cancer patients. *Br J Cancer* 2003;89:1638–44.
3. Leung W, Sandlund JT, Hudson MM, Zhou Y, Hancock ML, Zhu Y, et al. Second malignancy after treatment of childhood non-Hodgkin lymphoma. *Cancer* 2001;92:1959–66.
4. Hasegawa T, Matsuno Y, Niki T, Hirohashi S, Shimoda T, Takayama J, et al. Second primary rhabdomyosarcomas in patients with bilateral retinoblastoma: a clinicopathologic and immunohistochemical study. *Am J Surg Pathol* 1998;22:1351–60.
5. Bokemeyer C, Schmoll HJ. Secondary neoplasms following treatment of malignant germ cell tumors. *J Clin Oncol* 1993;11:1703–9.
6. Hartmann JT, Nichols CR, Droz JP, Horwich A, Gerl A, Fossa SD, et al. The relative risk of second nongerminal malignancies in patients with extragonadal germ cell tumors. *Cancer* 2000;88:2629–35.
7. Heyn R, Haeberlen V, Newton WA, Ragab AH, Raney RB, Tefft M, et al. Second malignant neoplasms in children treated for rhabdomyosarcoma. Intergroup Rhabdomyosarcoma Study Committee. *J Clin Oncol* 1993;11:262–70.
8. Scaradavou A, Heller G, Sklar CA, Ren L, Ghavimi F. Second malignant neoplasms in long-term survivors of childhood rhabdomyosarcoma. *Cancer* 1995;76:1860–7.
9. Pratt CB, Meyer WH, Luo X, Cain AM, Kaste SC, Pappo AS, et al. Second malignant neoplasms occurring in survivors of osteosarcoma. *Cancer* 1997;80:960–5.
10. Aung L, Gorlick RG, Shi W, Thaler H, Shorter NA, Healey JH, et al. Second malignant neoplasms in long-term survivors of osteosarcoma: Memorial Sloan-Kettering Cancer Center Experience. *Cancer* 2002;95:1728–34.
11. Merimsky O, Kollender Y, Issakov J, Bickels J, Flusser G, Gutman M, et al. Multiple primary malignancies in association with soft tissue sarcomas. *Cancer* 2001;91:1363–71.
12. Fletcher CDM, Unni KK, Mertens F, eds. World Health Organization Classification of Tumours. Pathology and Genetics of Tumours of Soft Tissue and Bone. Lyon, France: IARC Press;2002.
13. Hasegawa T, Yamamoto S, Yokoyama R, Umeda T, Matsuno Y, Hirohashi S. Prognostic significance of grading and staging systems using MIB-1 score in adult patients with soft tissue sarcoma of the extremities and trunk. *Cancer* 2002;95:843–51.
14. Kuttesch JF Jr, Wexler LH, Marcus RB, Fairclough D, Weaver-McClure L, White M, et al. Second malignancies after Ewing's sarcoma: radiation dose-dependency of secondary sarcomas. *J Clin Oncol* 1996;14:2818–25.
15. Rich DC, Corpron CA, Smith MB, Black CT, Lally KP, Andrassy RJ. Second malignant neoplasms in children after treatment of soft tissue sarcoma. *J Pediatr Surg* 1997;32:369–372.
16. Green DM, Hyland A, Barcos MP, Reynolds JA, Lee RJ, Hall BC, et al. Second malignant neoplasms after treatment for Hodgkin's disease in childhood or adolescence. *J Clin Oncol* 2000;18:1492–9.
17. Fletcher CD, Gustafson P, Rydholm A, Willen H, Akerman M. Clinicopathologic re-evaluation of 100 malignant fibrous histiocytomas: prognostic relevance of subclassification. *J Clin Oncol* 2001;19:3045–50.
18. Coindre JM, Terrier P, Guillou L, Le Doussal V, Collin F, Ranchere D, et al. Predictive value of grade for metastasis development in the main histologic types of adult soft tissue sarcomas: a study of 1240 patients from the French Federation of Cancer Centers Sarcoma Group. *Cancer* 2001;91:1914–26.
19. Mentzel T, Calonje E, Wadden C, Camplejohn RS, Beham A, Smith MA, et al. Myxofibrosarcoma. Clinicopathologic analysis of 75 cases with emphasis on the low-grade variant. *Am J Surg Pathol* 1996;20:391–405.
20. Weiss SW, Goldblum JR (2001) Fibrosarcoma. In: Enzinger and Weiss's Soft Tissue Tumours, 4th edn. St Louis: Mosby; 2001:423–5.

21. Huang HY, Lal P, Qin J, Brennan MF, Antonescu CR. Low-grade myxofibrosarcoma: a clinicopathologic analysis of 9 cases treated at a single institution with simultaneous assessment of the efficacy of 3-tier and 4-tier grading systems. *Hum Pathol* 2004;35:612–21.
22. Li FP, Fraumeni JF Jr. Prospective study of a family cancer syndrome. *J Am Med Assoc* 1982;247:2692–4.
23. Malkin D, Jolly KW, Barbier N, Look AT, Friend SH, Gebhardt MC, et al. Germline mutations of the p53 tumor-suppressor gene in children and young adults with second malignant neoplasms. *N Engl J Med* 1992;326:1309–15.
24. Kony SJ, de Vathaire F, Chompret A, Shamsaldim A, Grimaud E, Raquin MA, et al. Radiation and genetic factors in the risk of second malignant neoplasms after a first cancer in childhood. *Lancet* 1997; 350:91–5.
25. Chaplain G, Milan C, Sgro C, Carli PM, Bonithon-Kopp C. Increased risk of acute leukemia after adjuvant chemotherapy for breast cancer: a population-based study. *J Clin Oncol* 2000;18:2836–42.
26. Huang J, Mackillop WJ. Increased risk of soft tissue sarcoma after radiotherapy in women with breast carcinoma. *Cancer* 2001;92:172–80.

Original Report

Ukihide Tateishi[1]
Tadashi Hasegawa[2]
Hiroaki Onaya[1]
Mitsuo Satake[1]
Yasuaki Arai[1]
Noriyuki Moriyama[1]

Myxoinflammatory Fibroblastic Sarcoma: MR Appearance and Pathologic Correlation

OBJECTIVE. The purpose of our study was to define the MR appearance of myxoinflammatory fibroblastic sarcoma of the soft tissues and to make correlations with the histopathologic features.

CONCLUSION. Myxoinflammatory fibroblastic sarcoma is an uncommon malignancy that typically affects adult subjects, who present with painless swelling. This lesion manifests on MR images as a poorly circumscribed mass involving the underlying tendon sheath in the distal extremities.

Myxoinflammatory fibroblastic sarcoma of the soft tissues is a rare low-grade tumor of uncertain origin that usually arises in the hands and feet. Myxoinflammatory fibroblastic sarcoma was first described in 1998 by Meis-Kindblom and Kindblom [1]. Montgomery et al. [2] named the tumor "inflammatory myxohyaline tumor" of the distal extremities with virocyte or Reed-Sternberg-like cells. Histologic characteristics are the spindle to epithelioid neoplastic cells as the manifestation of malignancy admixed with the myxoid and hyalinized matrix, the inflammatory infiltrate, and bizarre virocyte or Reed-Sternberg-like cells with enlarged vesicular nuclei [1–3].

More than 100 cases of myxoinflammatory fibroblastic sarcoma have been reported, with a large series identified in two articles [1–6]. However, MRI findings of myxoinflammatory fibroblastic sarcoma have rarely been documented. The purpose of this study was to characterize the MR appearance of myxoinflammatory fibroblastic sarcoma and to correlate that appearance with the histopathologic features.

Materials and Methods

MR images of all patients with pathologically proven myxoinflammatory fibroblastic sarcoma at our institution were retrospectively reviewed. Our institutional review board gave its approval for a review of patient records and images. The patients were identified by review of our institution's pathology database for a 2-year period. The affected patients included three males and one female who ranged in age from 15 to 62 years old (mean age, 35 years). All histopathologic specimens were reviewed by an experienced pathologist to confirm the diagnosis. Histopathologic examination in all patients showed spindle and epithelioid tumor cells with mild nuclear atypia. Ganglionlike cells and Reed-Sternberg-like cells were also prominent in all cases. Inflammatory cells, including neutrophils, lymphocytes, and eosinophils, were densely present in all cases. Immunohistochemistry was performed in all patients, and all tumors displayed immunoreactivity to vimentin, smooth-muscle actin, and CD34. These histopathologic characteristics were compatible with the diagnosis of myxoinflammatory fibroblastic sarcoma [7]. Medical records were reviewed by one of the authors for presenting complaints, disease progression, and outcome. Radiographs, available for all patients, were also evaluated by two radiologists for the presence of soft-tissue masses or nodules, mineralization, and bone destruction. The findings were recorded by consensus.

T1- and T2-weighted MR images were obtained in the sagittal and coronal planes using a surface coil. T1-weighted conventional spin-echo MR images were obtained using a 20-cm field of view, 3.5- to 5-mm section thickness, TR range/TE of 450–520/15, 160 × 256 matrix, and 2 signals acquired. T2-weighted fast spin-echo acquisitions with (n = 3) or without (n = 1) fat suppression were performed using a 20-cm field of view, 3.5- to 5-mm section thickness, 3,600–4,000/120, 160 × 256 ma-

Received June 2, 2004; accepted after revision July 28, 2004.

Supported in part by grant for Scientific Research Expenses for Health and Welfare Programs, The Foundation for the Promotion of Cancer Research, and second-term Comprehensive 10-year Strategy for Cancer Control.

[1]Division of Diagnostic Radiology, National Cancer Center Hospital and Institute, Tsukiji, Chuo-Ku, 104-0045, Tokyo, Japan. Address correspondence to U. Tateishi.

[2]Pathology Division, National Cancer Center Hospital and Institute, Tsukiji, Tokyo, Japan.

AJR 2005;184:1749–1753

0361–803X/05/1846–1749

trix, and 2 signals acquired. After the IV administration of 0.1 mmol of gadopentetate dimeglumine (Magnevist, Schering) per kilogram of body weight, transverse T1-weighted images with ($n = 3$) or without ($n = 1$) fat suppression were obtained in the sagittal and coronal planes.

MR images were reviewed by two radiologists and findings were recorded by consensus. Images were evaluated for lesion location and size, depth (superficial or deep), shape of margin (well or ill defined), and the presence or absence of extracompartmental extension. To define depth, superficial lesions did not involve the superficial fascia, and deep lesions were deep in relation to or invaded the superficial fascia. The relationship between tumor and the underlying tendon sheath was also evaluated. MR images were evaluated for predominant signal intensity characteristics (low, intermediate, high), signal homogeneity or heterogeneity, and enhancement characteristics. On T1-weighted images, low signal intensity was defined as signal intensity less than that of muscle; intermediate signal intensity, similar to that of muscle; and high signal intensity, similar to that of fat. On T2-weighted images, low signal intensity was defined as signal intensity similar to that of muscle; intermediate signal intensity, greater than that of muscle but less than that of fat; and high signal intensity, equal to or greater than that of fat. Tumor enhancement was visually graded as greater than, less than, or equal to that of surrounding muscle and vessels.

Results

Clinical Features

All patients were symptomatic at presentation. Presenting complaints were painless swelling of the distal extremities. The mean symptom duration was 4.8 months. Tumors arose from the feet ($n = 2$), hands ($n = 1$), and fingers ($n = 1$). All patients received excisional biopsy for definitive diagnosis and primary therapy. Surgical margins were adequate in three patients and inadequate in one patient. The one patient with an inadequate surgical margin underwent subsequent wide resection. Chemotherapy and radiation therapy were not included in the treatment regimen in any patient. Local recurrence occurred 26.5 months after the initial surgery in two patients. These patients received wide resection. At the latest follow-up (27–82 months; mean, 45 months), no patients had developed further recurrence or metastasis.

MRI Findings and Pathologic Correlations

The gross characteristics of the resected specimens featured multinodular architecture corresponding to MRI features. The mean tumor diameter was 2.4 cm (range, 1.2–3.0 cm). Tumors were located along the tendon sheath in all patients. Findings of extensive involvement surrounding the tendon sheath by the tumor were seen. In two patients, the tumor existed beneath the tendon sheath (Fig. 1), and in two it involved the surrounding tendon sheath diffusely and focally infiltrated the dermis (Fig. 2). One patient had an ill-defined, irregularly marginated mass involving the ulnar nerve and the tendon sheath of the flexor carpi ulnaris (Fig. 2).

Cortical invasion was not identified in any patient on radiographs. All tumors showed predominantly low signal intensity relative to muscle on T1-weighted MR images (Fig. 3). Two lesions showed moderate and homogeneous enhancement after the IV administration of contrast material (Figs. 1 and 3). The cut surface of resected specimens showed solid nests of neoplastic cells that featured spindle and epithelioid cells with higher cellularity, which corresponded to homogeneous enhancement on contrast-enhanced MR images. Two lesions showed heterogeneous enhancement of the tumor that correlated with geographic areas of the myxoid stromal matrix on microscopic observations (Fig. 4). On T2-weighted MR images, all lesions had intermediate signal intensity greater than that of muscle but less than that of fat (Fig. 2). In all cases, the cut surface of specimens revealed solid nests of cellular areas with foci of hyalinized collagen fibers and hypocellular areas with a myxoid stromal

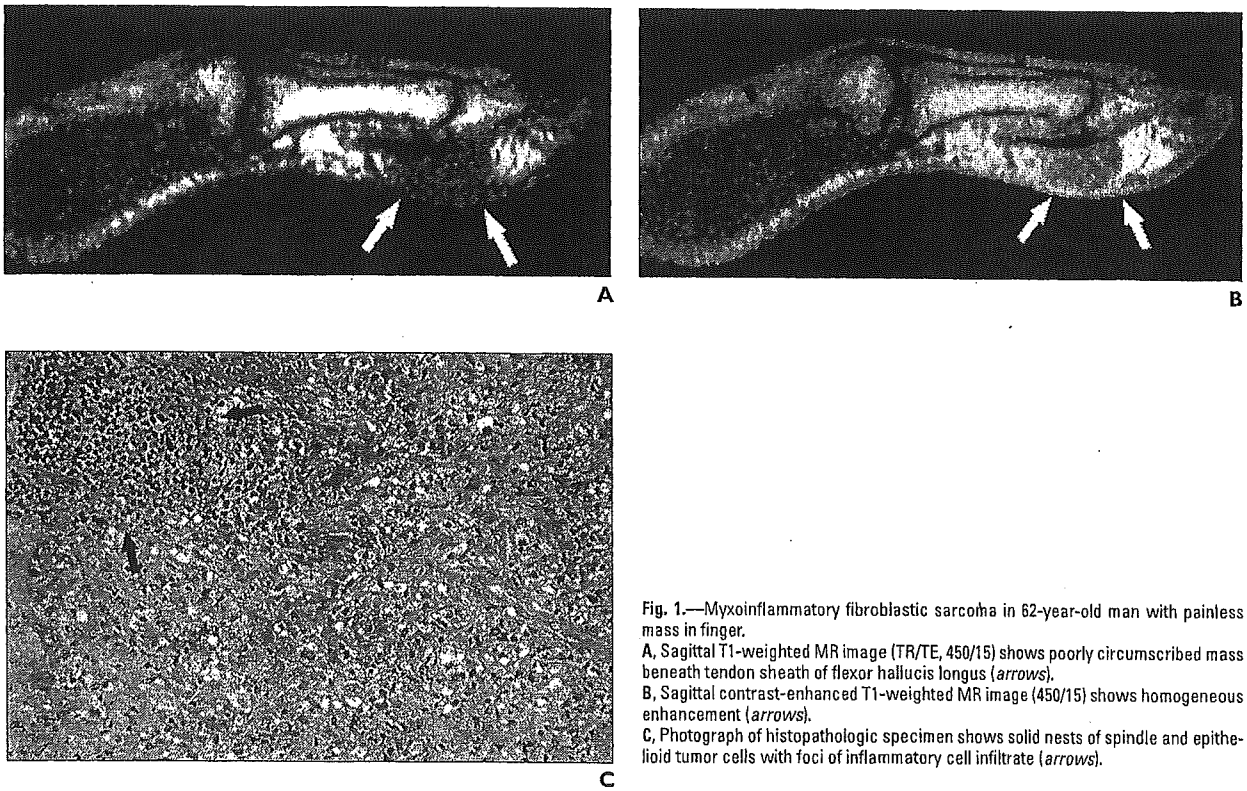

Fig. 1.—Myxoinflammatory fibroblastic sarcoma in 62-year-old man with painless mass in finger.
A, Sagittal T1-weighted MR image (TR/TE, 450/15) shows poorly circumscribed mass beneath tendon sheath of flexor hallucis longus (*arrows*).
B, Sagittal contrast-enhanced T1-weighted MR image (450/15) shows homogeneous enhancement (*arrows*).
C, Photograph of histopathologic specimen shows solid nests of spindle and epithelioid tumor cells with foci of inflammatory cell infiltrate (*arrows*).

matrix, which corresponded to the imaging appearance of intermediate signal intensity on T2-weighted MR images.

Two patients developed recurrent tumors and underwent follow-up MRI after treatment. One patient developed a mass of sheetlike appearance beneath the dorsal portion of the underlying tendon sheath (Fig. 3). Signal characteristics and homogeneous enhancement patterns were similar to those of the primary tumors. Histopathologic examination of this patient showed an infiltrate of lymphoid cells and a marked proliferation of spindle-shaped tumor cells surrounding the tendon sheaths.

In the second patient, a mass of branching pattern occurred along the extensor digitorum longus tendon sheaths of the second and fourth toes without distortion of the architecture of the tendon sheaths (Fig. 4). This patient had also MRI findings suggesting capsular involvement in the metatarsophalangeal joint of the second toe. Histopathologic examination revealed that the tumor arose from the extensor digitorum longus tendon sheaths and also involved the extensor digitorum brevis tendon sheath, cutaneous nerve, and dermis.

Discussion

Myxoinflammatory fibroblastic sarcoma is a rare tumor of the subcutaneous soft tissue that can arise on the trunk but most commonly occurs in the distant extremities [1, 2]. According to the literature and our experience, myxoinflammatory fibroblastic sarcoma is a tumor that most commonly affects adults who are symptomatic at presentation [1, 2]. All patients in our series were symptomatic, with common complaints of a painless mass.

Myxoinflammatory fibroblastic sarcoma has a relatively good prognosis with a long life expectancy despite frequent local recurrence [1–3]. Two of our patients developed local recurrence, with an average duration of 26.5 months. According to the literature, the local recurrence rate in patients with myxoinflammatory fibroblastic sarcoma ranges from 22% to 67% [1, 2]. The metastasis rate in patients with myxoinflammatory fibroblastic sarcoma is uncertain. Metastases have been reported to develop in only a few cases [1].

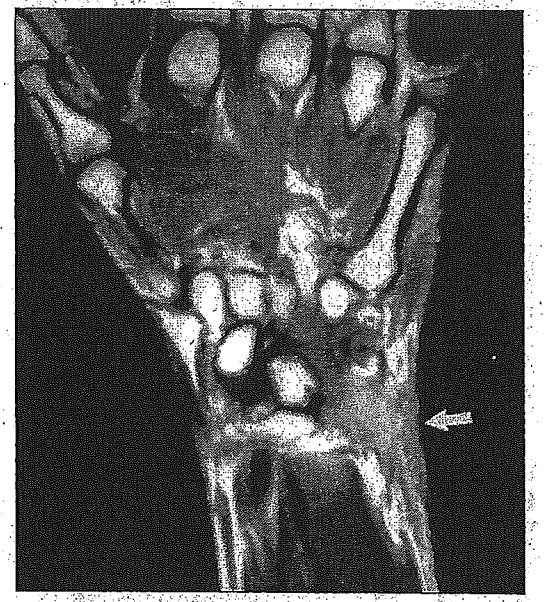

A

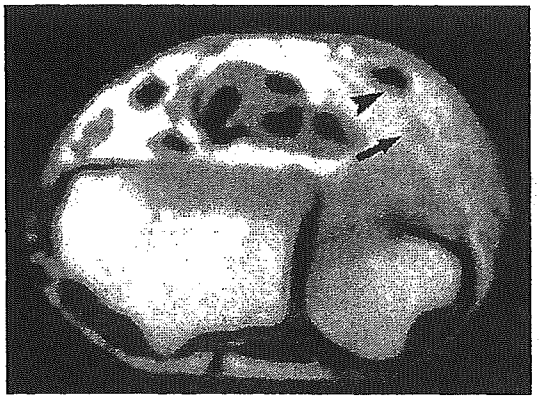

B

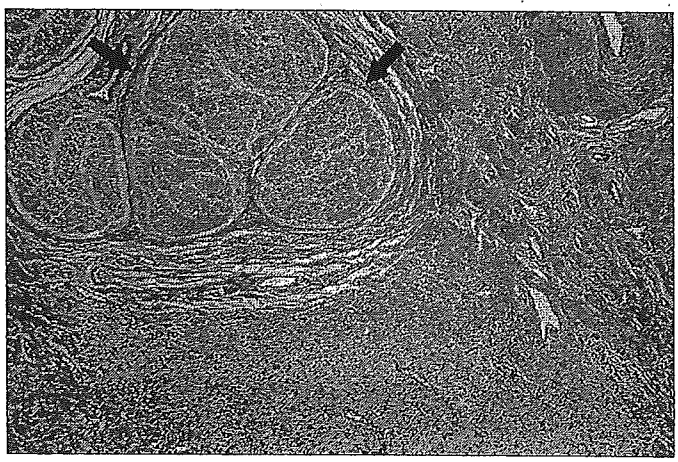

C

Fig. 2.—Myxoinflammatory fibroblastic sarcoma in 31-year-old man with painless mass in subcutaneous soft tissue of wrist.
A, Coronal contrast-enhanced T1-weighted MR image (TR/TE, 520/15) shows poorly circumscribed mass with ill-defined border. Tumor involves surrounding tendon sheath diffusely and focally infiltrates dermis (*arrow*).
B, Axial contrast-enhanced T1-weighted MR image (520/15) shows mass involving ulnar nerve (*arrow*) and tendon sheath of flexor carpi ulnaris (*arrowhead*).
C, Photograph of histopathologic specimen reveals that numerous small nodules consisting of tumor cells infiltrate along ulnar nerve (*arrows*).